IET Generation, Transmission & Distribution

IET Journals
The Institution of Engineering and Technology

Detection of Inconspicuous Power Quality Disturbances through Step Changes in rms Voltage Profile

ISSN 1751-8644
doi: 0000000000
www.ietdl.org

Alvaro Furlani Bastos [1,2] *Walmir Freitas* [3] *Grazia Todeschini* [4] *Surya Santoso* [1]

[1] *Department of Electrical and Computer Engineering, The University of Texas at Austin, Austin, TX 78712 USA*
[2] *CAPES Foundation within the Ministry of Education, Brasilia, 70040-031, Brazil*
[3] *Department of Electrical Energy Systems, University of Campinas, 13083-852, Campinas, SP, Brazil*
[4] *College of Engineering, Swansea University, Swansea SA1 8EN, UK*
* *E-mail: alvaro.fbastos@utexas.edu, walmir@dsee.fee.unicamp.br, grazia.todeschini@swansea.ac.uk, ssantoso@mail.utexas.edu*

Abstract: Power quality disturbances commonly observed in power systems have been studied for decades, resulting in numerous algorithms for detecting the events that affect the voltage and/or current waveforms. However, a considerable amount of disturbances are not visually observable in the raw waveforms, especially switching operations. These events must be detected through an alternative feature, such as abrupt variations in the rms voltage profile. This paper examines the methods commonly used for detecting power quality disturbances in the waveform or rms voltage profile domains and identifies their limitations. Afterwards, a novel step change detector is proposed based on a modified median filter and rms voltage gradient values to overcome the deficiencies of the existing methods. The effectiveness of the proposed method is assessed by applying it to both simulated and field data. This assessment shows that the method detects all switching events with no false-positives for the datasets under analysis.

1 Introduction

Power quality (PQ) disturbances have been a topic of interest to researchers and utilities for decades. Concerns with PQ problems tend to intensify with the increasing use of non-linear loads, electronic-based equipment, and inverter-interfaced distributed generation (especially photovoltaics) [1]. The widespread deployment of power quality monitors by multiple utilities and application of signal processing techniques allow further developments in the field of PQ disturbance analysis [2]. Even though new techniques and methodologies have been developed to identify and classify PQ disturbances, some issues are still challenging [3–5]. The most prominent example is the detection of PQ disturbances that are not directly observable in the raw voltage and/or current waveforms.

Analysis of PQ disturbances usually involves three steps: (i) signal analysis (de-noising and computation of derived quantities), (ii) feature selection, and (iii) disturbance classification [6]. A well-designed analysis in each step is essential for the performance of the subsequent steps.

The voltage and/or current waveforms during a PQ disturbance are valuable assets for power quality data analytics. However, these raw measurements might not directly provide useful information for disturbance identification and classification. In fact, various power system events may not cause conspicuous disturbances in the voltage and current waveforms; instead, they are characterised by an abrupt step change in the rms voltage profile. Such events include capacitor switching (especially the de-energizing operations) [7], transformer tap-changer operations, and switching of large loads [8].

Identification of these inconspicuous PQ disturbance events might be a complex task. A variety of methods is found in the literature to identify conspicuous disturbances, such as Fourier transform and short-time Fourier transform [9], wavelet transform [10, 11], S-transform [12–14], Kalman filtering [15–18], ESPRIT [19, 20], residuals of AR models [21], and residuals of harmonic models [22]. However, none of these methods is suitable for analysis of inconspicuous disturbances. Moreover, the rms voltage variation resulting from the switching events cited previously commonly fall within the normal voltage range, and are undetected by traditional sag/swell identification methods.

Therefore, rms voltage step changes are an alternative triggering feature that simplifies the identification of switching events. They also constitute a data reduction technique, where the raw voltage and current waveforms are thoroughly analysed only if a step change has been detected. This process reduces the time and computational effort for the analysis of triggerless power quality data.

Given the limitations mentioned earlier, this paper proposes a novel PQ disturbance detection technique, which uses rms voltage step changes as an alternative triggering feature and is able to detect subtle variations. Initially, the rms voltage profile is computed as a derived quantity from the raw voltage waveforms. The de-noising process of the resulting rms voltage profile is performed by a modified version of the median filter. This new filter is able to significantly attenuate the noise in the rms voltage profile while preserving the sharp edges caused by the switching events. Once filtered, the rms voltage profile is used to detect step changes based on rms voltage gradient values and a pre-specified threshold.

The paper is organised as follows. Section 2 discusses the most commonly used techniques for detection of PQ disturbances, which are based on a time-frequency decomposition of the waveforms, and concludes that these techniques are not applicable to the analysis of inconspicuous PQ disturbances. Section 3 proposes the step changes in an rms voltage profile as an alternative feature for detecting these types of PQ disturbances. It introduces the recommended approach for obtaining the rms voltage profile from the raw data and techniques to filter it. Moreover, this section examines two methods commonly used for detection of rms voltage step changes; synthetic and field voltage waveform data are employed to illustrate their limitations, even under proper selection of the algorithm parameters. Section 4 presents the novel technique for filtering the rms voltage profile, which is a modified version of the two-model approach and median filtering, and the corresponding technique for rms voltage step change detection. Considerations about the practical implementation of this detection method are discussed. The performance of the proposed method is demonstrated through simulated and field data in Section 5. Moreover, this section examines the benefits of employing voltage rather than current data for detection of inconspicuous switching events. Final considerations are addressed in Section 6.

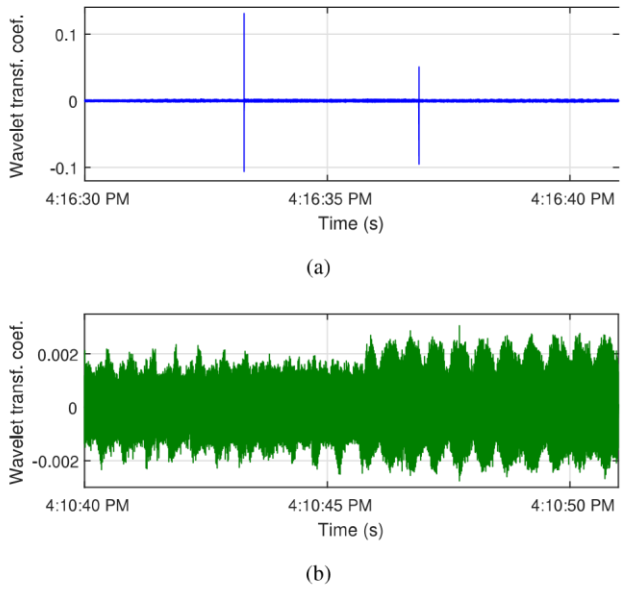

Fig. 1: Wavelet transform coefficients of the voltage waveform during capacitor switching operations. (a) Energizing. (b) De-energizing.

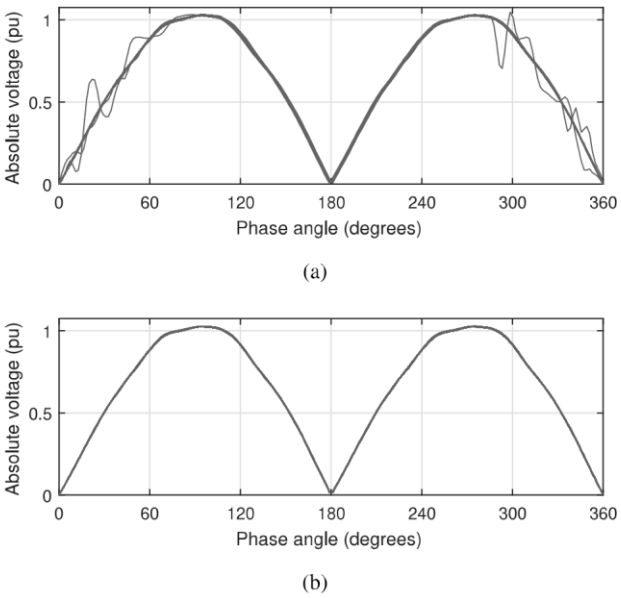

Fig. 2: Superimposed cycles of voltage waveform data (absolute values) for a 30-second measurement interval during capacitor switching operations. (a) Energizing. (b) De-energizing.

2 Literature Review

Analysis of PQ disturbances generally involves a time-frequency decomposition of the original signal. Fourier transform is a well-known technique for decomposing a signal into its harmonic components. Although it has been commonly applied for analysis of voltage and current waveforms, it assumes that the signal is stationary, which is not true during PQ disturbances. Therefore, this technique is not suitable for analyzing abrupt changes in the voltage and/or waveform data [3].

Many techniques have been proposed to resolve this issue, such as short-time Fourier transform, S-transform and Kalman filtering. Among these techniques, the wavelet transform became the most popular in the PQ field. It is implemented as a set of low-pass and high-pass filters, and the frequency resolution increases at each successive decomposition level [23]. This transform has been successfully applied to detect rapid changes in voltage and/or current waveforms (e.g. switch transients and voltage sags) [3, 10]; however, it fails when the underlying system event does not create a disturbance in the waveforms [24]. Another issue with the wavelet transform is the increased computational burden if multiple decomposition levels are required, posing a serious limitation for real-time operation of DSP-based instruments [25].

Given its popularity, the wavelet transform is chosen to illustrate the limitation of time-frequency signal decomposition techniques for analysis of inconspicuous disturbances. Fig. 1 depicts the wavelet transform coefficients of a voltage waveform during capacitor energizing and de-energizing operations; the mother wavelet is Daubechies 4 [7]. The high-frequency voltage transients caused by a capacitor energizing translate into severe spikes in the wavelet transform coefficients, as can be observed in Fig. 1a. On the other hand, the transient-free capacitor de-energizing operation results in a minor rise in the values of these coefficients, as shown in Fig. 1b. However, this increase is not sufficient to detect them as outliers, i.e. this PQ event is undetectable through the wavelet transform coefficients.

More in general, time-frequency decomposition techniques are applicable only to PQ disturbances that create a conspicuous anomaly in the waveforms. Fig. 2 represents superimposed cycles of voltage waveform data for a 30-second measurement interval (absolute values for around 1800 cycles), corresponding to the same capacitor switching events depicted in Fig. 1. While the capacitor energizing transients are clearly distinguishable, no voltage waveform variation is observable for the de-energizing operation. In other words, no PQ disturbance is detectable from the point of view of the waveforms only in Fig. 2b, and, therefore, a derived feature is needed for detecting the de-energizing event.

Inconspicuous PQ disturbances caused by events such as capacitor de-energizing, transformer tap-changer operations, and switching of large loads are characterised by a step change variation in the rms voltage profile. Therefore, the identification of step changes in an rms voltage profile allows detecting and classifying these disturbances. Even though this task appears simple, it may result in multiple false-negative classifications if the rms voltage profile is not properly pre-processed.

The magnitude of the rms voltage step changes due to inconspicuous PQ disturbances might be significantly small (even lower than 0.5% of the nominal voltage). Such small values are commonly hidden in the superimposed background noise, and, therefore, undetectable. To resolve this shortcoming, the following sections present an approach to process an rms voltage profile and detect even subtle step changes.

3 Traditional rms Voltage Step Change Detector

The most straightforward approach to detect inconspicuous switching events in power systems is through a time-dependent rms sequence. This section examines the standardised procedure to obtain an rms voltage profile, and its application in the detection of rms voltage step changes.

3.1 The rms Voltage Profile

According to industrial standards, rms voltage values must be computed from the sampled instantaneous voltage data over one-cycle long sliding windows and updated every half cycle [26–28]. The rms voltage sequence is denoted V_{rms}, and its computation is implemented as shown in (1).

$$V_{rms}\left[\frac{kN}{2}\right] = \sqrt{\frac{1}{N}\sum_{p=(k-2)N/2+1}^{kN/2} v[p]^2} \qquad (1)$$

for $k = 2, 3, \ldots$, and where N is the number of samples per cycle of the voltage waveform data. The resulting discrete rms voltage profile

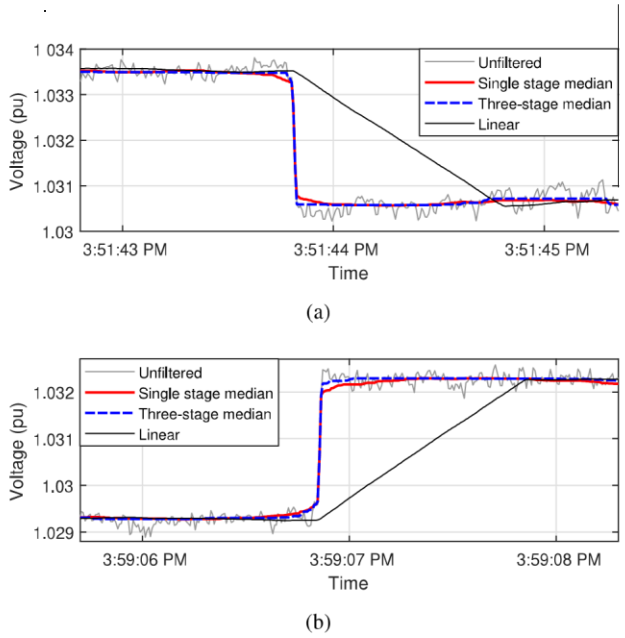

Fig. 3: Example of filtering an rms voltage profile with a linear filter ($M = 120$), and either single-stage ($M = 120$) or three-stage ($M_1 = 20$, $M_2 = 60$, $M_3 = 120$) median filters around rms voltage step changes. (a) Capacitor de-energizing. (b) Capacitor energizing.

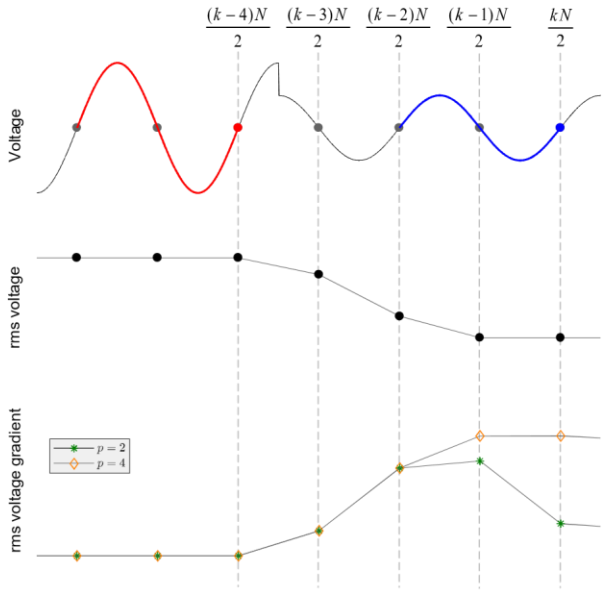

Fig. 4: Illustration of the voltage waveform data employed for computation of successive rms voltage values and rms voltage gradient profiles for $p = 2$ and $p = 4$.

assumes the shape of a stairstep graph, and its time resolution is half-cycle [24, 29].

3.2 Filtering of the rms Voltage Profile

The rms voltage profile computed according to (1) can be modeled as $V_{rms}(t) = \theta(t) + \varepsilon(t)$, where $\theta(t)$ is the deterministic component (the signal itself) and $\varepsilon(t)$ is additive noise. The noise component arises from the measuring device and a non-integer number of cycles within the rms sliding window; the latter factor is caused by the continuously time-varying power system frequency. Moreover, the rms voltage profile is non-smooth due to the intermittent load variation between consecutive rms voltage computations.

The standard approach to estimate the signal deterministic component in a noisy environment is low-pass filtering [30]. Linear filtering, such as the moving average filter over a fixed-length sliding window, is effective in removing or attenuating the rapid voltage fluctuations while preserving the slowly varying signal. However, it blurs out the signal edges [31, 32]. More precisely, when a moving average filter with length M is applied around an rms voltage step change, the filtered rms voltage profile gradually changes from the pre-step to the post-step voltage levels. This transition introduces $(M - 1)$ intermediary points between the two steady-state conditions [33].

It is well-documented in the literature that median filtering outperforms linear filtering in removing noise from a signal that contains sharp edges [32]. In fact, median filters are recognised to be robust against bias caused by data contamination [34, 35]. For a time sequence $X(t) = \{x_1, x_2, \ldots, x_n, \ldots\}$, the output of a median filter with length M at the index n is given by (2).

$$\widetilde{x}_n = \text{med}\left\{x_{n-\lceil \frac{M-1}{2} \rceil}, \ldots, x_n, \ldots, x_{n+\lfloor \frac{M-1}{2} \rfloor}\right\} \qquad (2)$$

where $\text{med}(\cdot)$ represents the median operator.

In the context of an rms voltage profile containing step changes, rms values near the edge contaminate the filtering process (post-step rms values affect filtering of pre-step rms values, and vice-versa). While linear filters are highly sensitive to this contamination, median filters can resist it. However, this superiority of median filters is observed only at large signal-to-noise ratios (low noise levels) [32].

An iterated and multiscale filtering approach can be used to overcome the limited superiority of median filters at high noise levels [32]. Median filters are applied sequentially over windows of different lengths, from a fine scale (narrow window) to a coarse scale (wide window). This process aims at increasing the signal-to-noise ratio at each stage to leverage the advantages of median filtering at increasingly lower noise levels.

It is important to emphasise that a similar approach is not applicable to linear filtering. In fact, the results of sequential iterated linear filtering can be achieved by a single linear filter with an appropriate kernel [32]. Therefore, both single-stage and iterated linear filtering have similar poor performance near the signal edges.

A three-stage median filtering is adopted in this work, as suggested in [32] for noisy signals that contain sharp edges. The window lengths are chosen as $M_1 = 20$, $M_2 = 60$, and $M_3 = 120$, which correspond to 1/6, 1/2, and 1 second of the raw rms voltage profile, respectively. Fig. 3 illustrates the performance of single-stage and three-stage median filters in filtering the rms voltage profile around capacitor energizing and de-energizing operations. While both filters are able to significantly reduce the rapid voltage fluctuations, the three-stage median filter presents a faster transition from pre-step to post-step voltage levels. This figure also illustrates that linear filters are not suitable for portions of the signal around step changes; note that the duration of the transition segment between pre-step and post-step voltage levels is equal to the filter length ($M = 120$ samples or 1 second in this case).

3.3 RMS Voltage Gradient

The simplest detection method of sudden rms voltage step changes uses the rate of change as the triggering criteria, and it is described through Fig. 4. Such an event is detected when the absolute difference between two rms voltage values exceeds a threshold, as shown in (3).

$$\Delta V_{rms} = \left| \widetilde{V}_{rms}\left[\frac{kN}{2}\right] - \widetilde{V}_{rms}\left[\frac{(k-p)N}{2}\right] \right| > \delta_{step} \qquad (3)$$

where $\widetilde{V}_{rms}$ is the *filtered* rms voltage profile, δ_{step} is the prespecified threshold, and p is the number of steps back in time in the rms voltage sequence. Note that increasing p by one unit moves the rms sliding window backwards by a half-cycle over the voltage waveform data, as can be observed in Fig. 4.

It has been recommended to adopt $p = 2$ [8]; however, this value might not be appropriate for all situations. The rms voltage values at

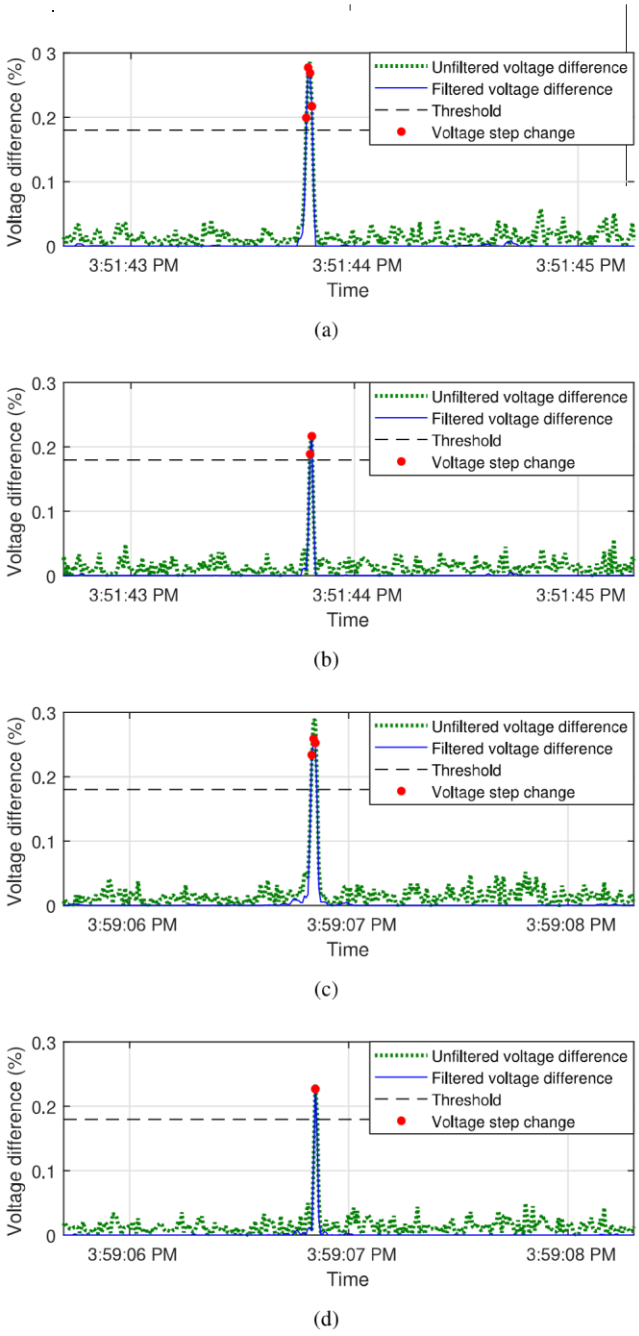

Fig. 5: Example of the rms voltage gradient for unfiltered and filtered rms voltage profiles. (a) Capacitor de-energizing ($p = 4$). (b) Capacitor de-energizing ($p = 2$). (c) Capacitor energizing ($p = 4$). (d) Capacitor energizing ($p = 2$).

$kN/2$ and $(k-2)N/2$ utilise adjacent cycles of the voltage waveform, as illustrated in Fig. 4. If an rms voltage step change occurs within one of those cycles, the corresponding rms voltage value is between the pre-step and post-step voltage levels, as illustrated in the rms voltage gradient profile for $p = 2$ in Fig. 4. Therefore, the resulting ΔV_{rms} value is smaller than the true size of the rms voltage step, and the event may be undetected. This work adopts $p = 4$, such that there is a one-cycle gap of voltage waveform data between the two rms voltage values. It allows the dissipation of possible transients caused by the switching event and guarantees that the total size of the voltage step change is correctly obtained, as shown by the gradient profile for $p = 4$ in Fig. 4.

3.3.1 Threshold selection: An appropriate choice for the threshold δ_{step} is essential to improve the detector performance. False alarms might occur if δ_{step} is too small and the detector is triggered by frequent load changes; on the other hand, step change event underdetection occurs if δ_{step} is too large.

The selection of the threshold is based on the most subtle switching events observed in power systems, as discussed below.

- Voltage regulators: these devices allow to adjust the voltage level by changing the tap positions in an autotransformer [36]. They commonly provide a range from -10% to +10% with 32 steps, so that each step corresponds to $\pm 0.625\%$ of the nominal voltage [37].
- Capacitor banks: the steady-state voltage variation (ΔV) caused by capacitor switching depends on the capacitor bank size (Q_C) and the short-circuit capacity (S_{sc}) at the bank location. This voltage variation, given as a percentage of the nominal value, can be approximated as [38]:

$$\Delta V = \frac{Q_C}{S_{sc}} \times 100\% \approx \left(\frac{f_{system}}{f_s}\right)^2 \times 100\% \tag{4}$$

where f_{system} is the system power frequency in Hz, and f_s is the switching transient frequency in Hz. The magnitude of the voltage variation computed through this equation is valid for all locations downstream the capacitor bank. The upstream locations also experience a voltage rise; however, the voltage rise magnitude varies from ΔV (at the bank location) to zero (at the substation) [37]. The frequency of capacitor energizing transients commonly falls in the range 300 Hz - 1000 Hz, such that the corresponding voltage variation is between 0.36% and 4% for a 60 Hz system.

As a rule of thumb, the threshold δ_{step} is chosen as half of the minimum expected step change [30]. Therefore, this work adopts $\delta_{step} = 0.0018$ pu.

3.3.2 Results: Fig. 5 illustrates the ΔV_{rms} profiles for the capacitor switching events analysed in Fig. 3 for $p = 2$ and $p = 4$. Red dots correspond to the rms voltage gradient values that exceed the threshold δ_{step}; note that any single event might contain up to p consecutive of such points. Both switching events were detected using either unfiltered or filtered rms voltage profiles, and either p value. However, it is not possible to generalise this result to all unfiltered voltage profiles. For example, note in Figs. 5b and 5d that using $p = 2$ does not allow to obtain the true size of the step changes, as discussed previously, and ΔV_{rms} in both cases were only slightly above the threshold. Moreover, the magnitude of the step change in Fig. 5c would be overestimated by the unfiltered rms voltage profile even with $p = 4$ (the incorrect rms voltage gradient values in this instance are due to the voltage waveform transients caused by the capacitor energizing operation). Therefore, applying a filtering approach for the rms voltage profile is highly recommended. Median filtering, however, is not applicable to all plausible rms voltage profiles, as will be discussed in the following section.

3.4 Alternative Standard Detector

An rms voltage step change is denominated *rapid voltage change* (RVC) in [26]. This standard proposes to detect an RVC event based on the rms voltage profile computed as (1). An rms voltage value is assumed to represent a quasi-steady-state condition if the difference between its value and the arithmetic mean of the immediately preceding 120 (60 Hz system) or 100 (50 Hz system) rms voltage values does not exceed an user-specified threshold (δ_{IEC}). Mathematically, an RVC event occurs at the instant n when the inequality in (6) is satisfied (for a 60 Hz system).

$$V_{avg,IEC}[n] = \frac{1}{120} \sum_{p=n-119}^{n} V_{rms}[p] \tag{5}$$

$$|V_{rms}[n] - V_{avg,IEC}[n]| > \delta_{IEC} \tag{6}$$

where δ_{IEC} and the rms voltage values are in pu. The computations in (5) and (6) are repeated whenever a new rms voltage value is available. The standard recommends adopting $0.01 \text{ pu} \leq \delta_{IEC} \leq 0.06$ pu, which is chosen according to the application. This technique is similar to linear filtering, which, as discussed previously, blurs out the signal edges.

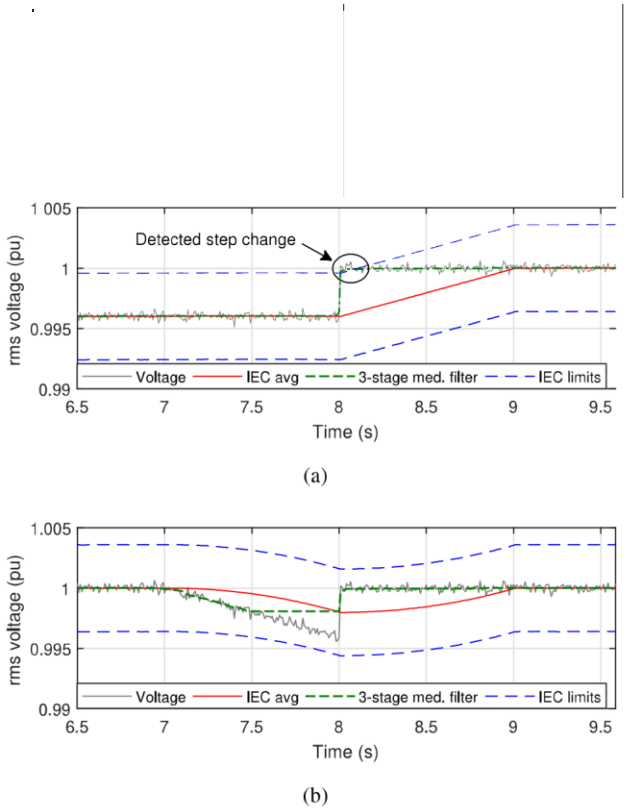

Fig. 6: Illustration of an RVC event detection with $\delta_{IEC} = 0.0036$ pu. (a) Detected RVC. (b) Undetected RVC.

To facilitate the discussion, two examples of capacitor switching will be analysed as follows:

1. A distribution system is in quasi-stationary state at a voltage level of 0.996 pu. At $t = 8$ s, a capacitor bank is energized, instantaneously increasing the rms voltage to 1 pu (an increase of 0.4% of the nominal value), as represented in Fig. 6a.
2. A large amount of load is gradually connected into the system over 1 second, starting at $t = 7$ s. As a result, the rms voltage drops linearly 0.4% of the nominal value (from 1 pu to 0.996 pu), as represented during the time interval 7 s - 8 s in Fig. 6b. This voltage drop triggers the energizing of a capacitor bank at $t = 8$ s, instantaneously increasing the rms voltage by 0.4% of the nominal value.

The rms voltage values in Fig. 6 are sampled from a normal distribution with the specified mean and standard deviation of 0.00025 pu. Adopting $\delta_{IEC} = 0.0036$ pu, only the first switching event is successfully detected, even though the step change magnitude is the same in both cases (0.004 pu). The undetected rms voltage step change in Fig. 6b suggests that this technique performs reasonably well only when the segments of data immediately before and after the event correspond to quasi-steady-state conditions. This assumption, however, is not true in general. Also, note that the three-stage median filter proposed in Section 3.2 is not able to track the rms voltage signal in the second case (see Fig. 6b between 7.5 s and 8 s).

The analysis presented in this section highlighted the drawbacks of the commonly used methods for identification of rms voltage step changes. While the rms voltage gradient technique seems promising (assuming a suitable threshold selection), it would fail if the rms voltage profile is not properly filtered (as occurred with the three-stage median filter in Fig. 6b). On the other hand, the alternative standard detector is subjected to attenuation of the signal edges, as commonly observed in linear filtering.

The drawbacks of both methods are implicitly associated with the process of discriminating between the deterministic component and the additive noise in the rms voltage profile through low-pass filtering. Therefore, the following sections focus on the development of a novel filter that removes the rapid fluctuation of the rms voltage

4 Proposed Method

This section presents a novel procedure for filtering an rms voltage profile and detecting step changes through a modified version of the two-model approach. This detection technique assumes that the deterministic component $\theta(t)$ of $V_{rms}(t)$ is piecewise constant or slowly-varying most of the time. The time instants between adjacent segments of the piecewise constant sequence correspond to abrupt changes in $\theta(t)$. The detection problem is concerned with estimating the time instants τ_i where the magnitude of $\theta(t)$ suddenly changes from θ_i to θ_{i+1}, as represented in (7). Each time instant τ_i indicates a transition between two adjacent quasi-stationary segments of data.

$$V_{rms}(t) = \begin{cases} \theta_1 + \varepsilon(t), & \text{for } 0 < t \leq \tau_1 \\ \theta_2 + \varepsilon(t), & \text{for } \tau_1 < t \leq \tau_2 \\ \quad\vdots & \quad\vdots \\ \theta_k + \varepsilon(t), & \text{for } \tau_{k-1} < t \leq \tau_k \end{cases} \tag{7}$$

The underlying idea in the two-model approach is to analyse the similarity between the *current* model (ψ) and a *nominal* model (ψ_0). The current model is based on a segment of data containing M data samples, while the nominal model is obtained from another segment of data (some or all of the past data except the samples used to obtain the current model) or off-line analysis (system identification or physical modelling) [30]. In this work, the two-model technique is employed during the filtering process of the rms voltage profile, and both models are obtained from adjacent, non-overlapping segments of data with size M.

Consider the time series $Y_{rms}(t) = \{y_1, y_2, \ldots, y_{t'}, \ldots, y_t, \ldots\}$ represents the rms voltage profile computed as (1), where $y_{t'}$ is the rms data sample computed at the time instant under analysis (t'). Then, the models ψ_0 and ψ are obtained from the data samples within the reference ($\mathcal{R}$) and observation ($\mathcal{O}$) sliding windows, respectively, as defined in (8).

$$\ldots, \underbrace{y_{t'-M}, \ldots, y_{t'-2}, y_{t'-1}}_{\substack{\text{Reference window } (\mathcal{R}) \\ \text{Nominal model } (\psi_0) \\ M \text{ elements}}}, \underbrace{y_{t'}, y_{t'+1} \ldots, y_{t'+M-1}}_{\substack{\text{Observation window } (\mathcal{O}) \\ \text{Current model } (\psi) \\ M \text{ elements}}}, \ldots \tag{8}$$

For notational simplicity, these sliding windows at the time instant t' are redefined as follows:

$$\mathcal{R}(t') = (y_{t'-M}, \ldots, y_{t'-1}) = (r_1, r_2, \ldots, r_{M-1}, r_M) \tag{9}$$

$$\mathcal{O}(t') = (y_{t'}, \ldots, y_{t'+M-1}) = (o_1, o_2, \ldots, o_{M-1}, o_M) \tag{10}$$

where $r_1, \ldots, r_M$ and $o_1, \ldots, o_M$ are the M rms voltage samples within the reference and observation windows, respectively, ordered by increasing time.

The choice of the window size is a compromise between model accuracy and detection delay. While long sliding windows result in more accurate models, short windows are needed for quick detection (quasi-real-time analysis) [39]. Note that the time analysis is performed with a delay of $(M - 1)$ samples.

The proposed filtering procedure and detection of step changes in an rms voltage profile are described below.

4.1 Filtering of the rms Voltage Profile

As discussed previously, neither moving average nor median filters performs satisfactorily for rms voltage profiles that contain step changes. Given the time series $Y_{rms}(t)$, the goal is to obtain its filtered version ($y_{\text{filt}}(t)$) without affecting the step changes. The strategy proposed in this section is a modified version of a median filter, where the range of raw rms voltage values used by the median operator is determined according to the occurrence of a step change within either sliding window $\mathcal{R}(t')$ or $\mathcal{O}(t')$

There are three mutually exclusive possibilities for the location

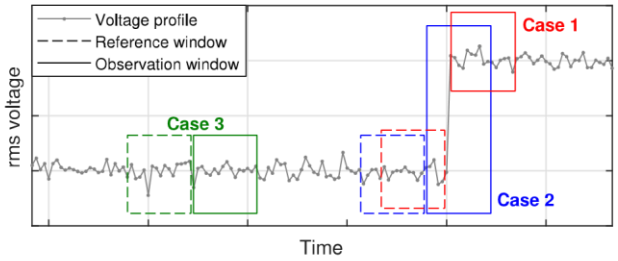

Fig. 7: Illustration of the possible locations of an rms voltage step change in relation to the reference and observation windows.

as described below. These three cases are illustrated in Fig. 7 (note: even though the reference and observation windows are adjacent at each time instant, a small gap has been introduced between them for better visualization).

- Case 1: an rms voltage step change occurs at t', such that the reference and observation windows correspond to pre-event and post-event data only, respectively. In such case, the filtered rms voltage value at the instant t' is determined by the post-event data samples (observation window), as shown in (11).

$$y_{\text{filt}}(t') = \text{med}(y_{t'}, \ldots, y_{t'+M-1}) = \text{med}(\mathcal{O}(t')) \quad (11)$$

An rms voltage step change at the time instant t' is detected through the median absolute deviation and it is presented in Section 4.1.1.

- Case 2: an rms voltage step change occurs within the observation window, posterior to t'. In this case, it is necessary to identify the index i^* where the possible step change happens, such that $1 < i^* < M$. Section 4.1.2 describes the procedure to determine this parameter.

A combination of samples from the reference and observation windows is used to compute the filtered rms voltage value, as shown in (12). Note that the samples selected from the observation window include only points prior to the possible step change.

$$y_{\text{filt}}(t') = \text{med}(\underbrace{y_{t'-i^*}, \ldots, y_{t'-1}}_{i^* \text{ samples from } \mathcal{R}(t')}, \underbrace{y_{t'}, \ldots, y_{t'+i^*-1}}_{i^* \text{ samples from } \mathcal{O}(t')}) \quad (12)$$

Although the whole reference window corresponds to pre-event data, only its last i^* samples are considered, i.e. the reference and observation windows contribute with the same number of samples to compute the filtered value. This condition is especially important if the pre-event data is slowly varying rather than in quasi-steady-state.

- Case 3: neither of the two sliding windows contain an rms voltage step change. The respective filtered rms voltage value is given as the median point of both windows, as represented in (13).

$$y_{\text{filt}}(t') = \text{med}(\underbrace{y_{t'-M}, \ldots, y_{t'-1}}_{\mathcal{R}(t')}, \underbrace{y_{t'}, \ldots, y_{t'+M-1}}_{\mathcal{O}(t')}) \quad (13)$$

The occurrence of these cases is analysed sequentially and the filtered rms voltage value at the time instant t' is defined by the first case identified (i.e. Case 1 has precedence over Case 2, which has precedence over Case 3). The proposed filtering technique is summarised in Fig. 8, and additional details regarding Case 1 and Case 2 are provided in the subsequent sections.

4.1.1 Case 1 and Median Absolute Deviation: An rms voltage step change detection at t' is based on the similarity between the models ψ_0 and ψ. This problem is formulated through the following hypotheses:

$$\begin{cases} \mathcal{H}_0 \text{ (no step change):} & \mathcal{M}(t') < \delta(t') \\ \mathcal{H}_1 \text{ (with step change):} & \mathcal{M}(t') \geq \delta(t') \end{cases} \quad (14)$$

where $\mathcal{M}(t')$ is a divergence measure between the models ψ_0 and ψ at the time instant t', and $\delta(t')$ is the adaptive threshold. An abrupt

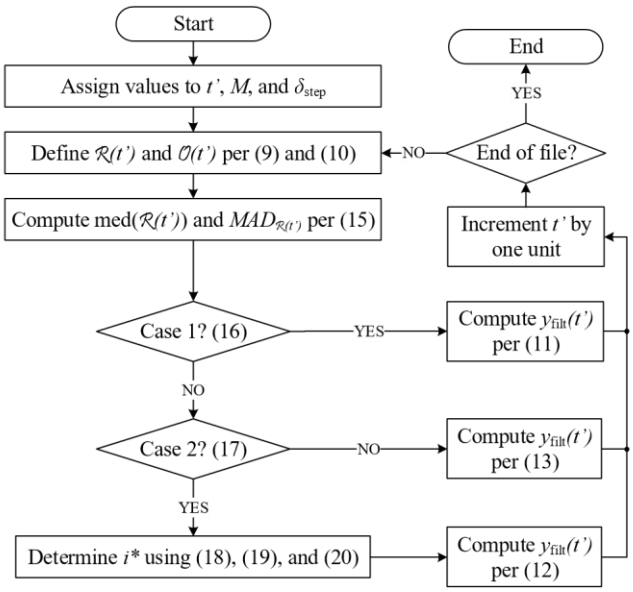

Fig. 8: Summary of the proposed filtering procedure.

change in the rms voltage data at t' is reflected as an inconsistency between the models ψ_0 and ψ. In other words, the data samples within the observation window behave as outliers compared to the model ψ_0. Under this condition, the null hypothesis $\mathcal{H}_0$ is rejected and a step change has been detected.

The goal of defining a threshold is to decide whether the growth in $\mathcal{M}(t')$ is significant. The threshold value represents a tradeoff between sensibility and robustness. The most ubiquitous approach for outlier detection is setting a threshold at ± 2 or ± 3 standard deviations around the dataset mean. However, this technique is unreliable as both mean and standard deviation are highly sensitive to the presence of atypical or incorrect data samples. An alternative consists in using the median and median absolute deviation (*MAD*, as defined in (15)), which are also a measure of central tendency while being mostly insensitive to the presence of outliers.

The robustness of an estimator against outliers is commonly assessed through the breakdown point [40]. This index is defined as the largest proportion of atypical points that the dataset may contain while the estimator still produces a correct result about the distribution of the typical points [41]. For a reasonable estimate, the dataset must contain more typical than atypical data samples; therefore, the breakdown point cannot exceed 0.5. For example, the breakdown points for the mean and median estimators are 0 and 0.5, respectively. Similarly, the *MAD* has a breakdown point of 0.5 and it is considered the most robust estimate of scale, while the classical interquartile range has a breakdown point of 0.25 only [42].

For an univariate dataset $X = \{x_1, x_2, \ldots, x_n\}$, the median absolute deviation (MAD_X) is defined as:

$$MAD_X = b \times \text{med}(|x_i - \text{med}(X)|), i = 1, 2, \ldots, n \quad (15)$$

where b is a scale factor needed for making the MAD_X a consistent estimator of the parameter of interest [42] (this factor depends on the underlying distribution). A previous study indicates that it is reasonable to assume that the rms voltage profile converges to a normal distribution during quasi-steady-state conditions [33]; in such case, $b \approx 1.4826$.

The reference window is used to determine the boundaries of expected values for the observation window. These values are computed through the Hampel identifier [43], which is the counterpart of using a given number of standard deviations around the mean, as shown in (16). An rms voltage step change occurred at t' if *all* observation samples exceed the threshold set by the Hampel identifier.

$$o_i \gtrless \text{med}(\mathcal{R}(t')) \pm r \times MAD_{\mathcal{R}(t')}, \forall i \in \{1, 2, \ldots, M\} \quad (16)$$

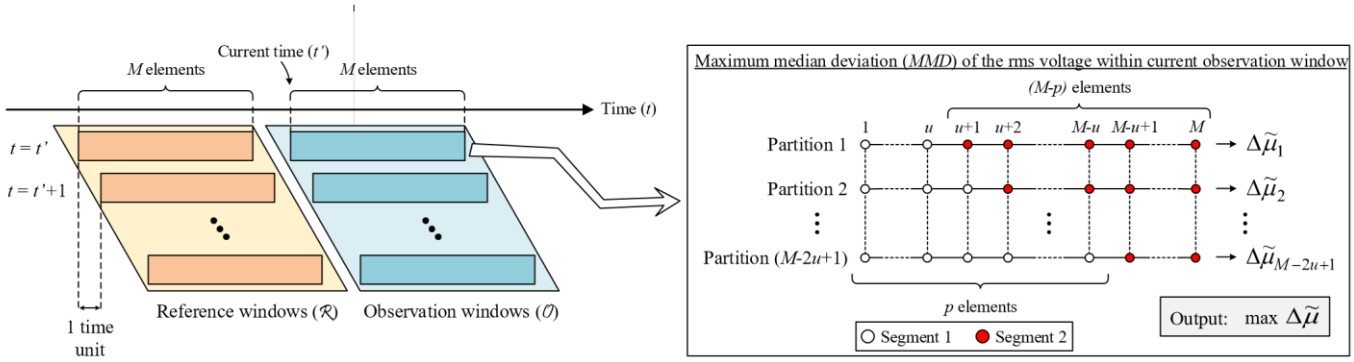

Fig. 9: Illustration of the multiple partitions of the observation window and computation of the maximum median deviation.

where $\mathcal{R}(t')$ and o_i are defined as in (9) and (10), respectively. The choice of the multiplicative factor r is subjective and regulates the sensitivity of the detector. In [44], r equals to 2 or 3 is suggested as a reasonable choice.

4.1.2 Case 2 and Maximum Median Deviation: The first step to detect a possible rms voltage step change within the observation window consists in computing the difference between the maximum and minimum values of the data points included in this sliding window. The observation window might contain a step change if, and only if, this difference exceeds a specified threshold, as represented in (17).

$$\max(\mathcal{O}(t')) - \min(\mathcal{O}(t')) > \delta_{step} \tag{17}$$

where δ_{step} is the threshold for rms voltage step change detection defined in Section 3.3.

Note, however, that this condition does not guarantee the occurrence of a step change within the observation window, as intermittent load variation might cause voltage fluctuations that satisfy the inequality above. This shortcoming is overcome by determining the maximum abrupt change within the observation window using a filtered version of the rms voltage profile.

The observation window is split into two non-overlapping, adjacent segments of data, $\mathcal{S}_1(p)$ and $\mathcal{S}_2(p)$, with lengths p and $(M-p)$, respectively, as defined in (18).

$$\begin{cases} \mathcal{S}_1(p) = (o_1, o_2, \ldots, o_p) \\ \mathcal{S}_2(p) = (o_{p+1}, \ldots, o_M) \end{cases} \quad \text{for } p = u, (u+1), \ldots, (M-u) \tag{18}$$

where $u = \max\{5, \lfloor M/8 \rfloor\}$. This constraint is imposed over u to prevent applying the median operator (see (19)) to very short segments of data, which could result in an estimator highly affected by outliers. According to this definition, a window with M samples has $(M - 2u + 1)$ unique partitions. The goal of this segmentation is to move p through the observation window to obtain a partition where $\mathcal{S}_1(p)$ contains only pre-step data and $\mathcal{S}_2(p)$ contains only post-step data.

For each partition p, the median of each segment is computed (this is equivalent to filtering each segment separately), and the absolute difference between them, $\Delta\tilde{\mu}(p)$, is defined as follows:

$$\Delta\tilde{\mu}(p) = |\text{med}(\mathcal{S}_1(p)) - \text{med}(\mathcal{S}_2(p))| \tag{19}$$

Finally, the possible step change within the observation window is assumed to have occurred at the index i^* where $\Delta\tilde{\mu}(p)$ is maximum, as shown in (20).

$$i^* = \arg\max\{\Delta\tilde{\mu}(p) | u \leq p < (M-u)\} \tag{20}$$

The quantity $\Delta\tilde{\mu}(i^*)$ is denominated *maximum median deviation*. Among all possible partitions defined by (18), the discrepancy between $\mathcal{S}_1(i^*)$ and $\mathcal{S}_2(i^*)$ is maximum, i.e. the possible step change within the observation window is most lik ly to have occurred at the index i^*. The procedure described in this section is illustrated in Fig. 9, where the left plot illustrates the reference and observation sliding windows for multiple time instants, and the right plot corresponds to the computation of the maximum median deviation for a specific time instant.

4.2 RMS Voltage Step Change Detection

Once the rms voltage profile has been filtered according to the procedure described above, resulting in the time sequence $y_{\text{filt}}(t)$, step changes are detected through the rms voltage gradient, as discussed in Section 3.3. For clarity, the test condition for step change detection at t' presented in (3) is repeated below.

$$\Delta V_{rms}(t') = |y_{\text{filt}}(t') - y_{\text{filt}}(t'-p)| > \delta_{step} \tag{21}$$

where p and δ_{step} are the same parameters defined in Section 3.3.

4.3 Voltage vs. Current Data

Theoretically, the filtering and detection techniques proposed in this paper can be used with either voltage or current data. However, a current step change is considered a power quality event only when the corresponding voltage step change is sufficient to trigger its detector [26]. Furthermore, some challenges arise when considering current data, as discussed below:

1. Current is more sensitive to load variations than the system voltage. For that reason, a large number of relatively small load variations may trigger the step change detector.
2. The expected magnitude of the rms current step change during a switching event is not well defined. This value is highly dependent on multiple characteristics of the system under analysis. Therefore, the value chosen for the parameter δ_{step} must be re-evaluated for each different system, i.e. the detector would have a poor generalization.
3. In the specific case of capacitor switching, an rms current step change is observed only for capacitor banks located downstream the monitoring location [7].

Therefore, the development of this technique assumes the use of voltage data only.

4.4 Practical Implementation Considerations

Modern PQ monitors are capable of real-time computation of parameters derived from the sampled voltage and current waveforms, such as rms values, harmonic distortion, active and reactive power, and power system frequency [45]. These parameters are commonly used as triggering features for detection and recording of PQ disturbances, such that only a few cycles of data before and after the disturbance are stored. The rms voltage step change proposed in this study has the potential to be used as a sophisticated trigger feature for detecting inconspicuous switching disturbances in real-time operation.

IET Generation, Transmission & Distribution, pp. 1–10

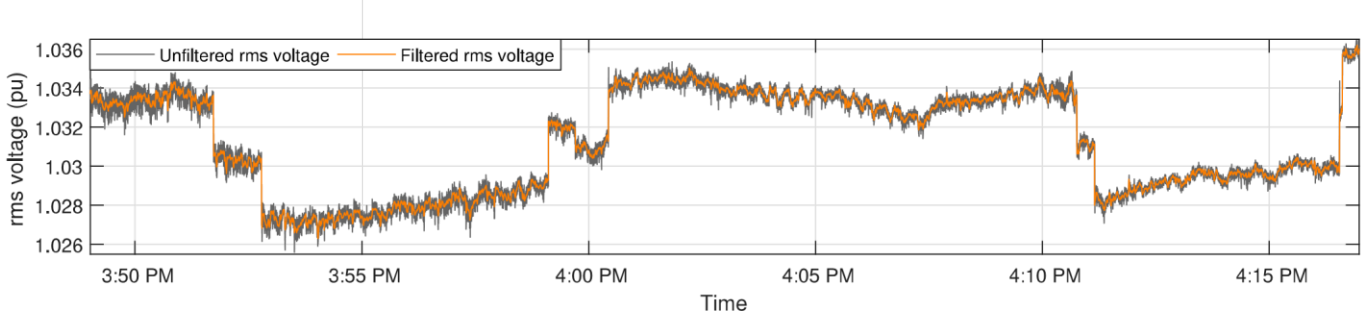

(a)

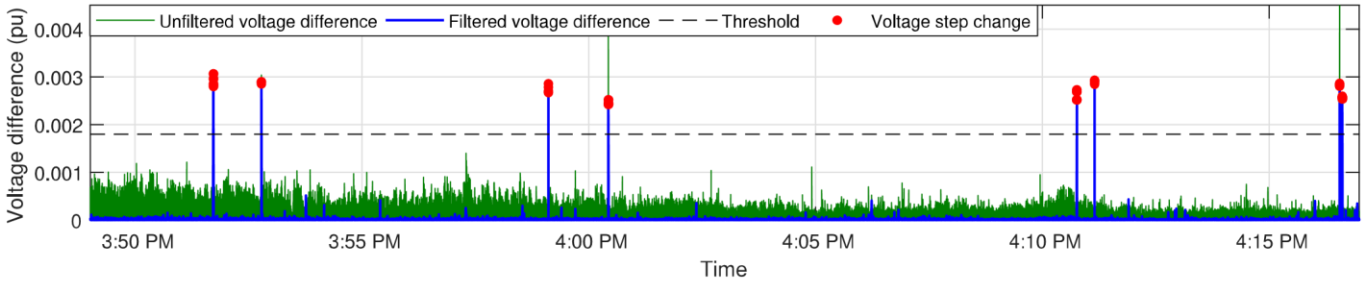

(b)

Fig. 10: Illustration of the proposed filtering and rms voltage step change detection techniques. (a) rms voltage profiles. (b) rms voltage gradient.

This method can be implemented for either off-line or on-line waveform data analysis. The on-line analysis is more challenging, as PQ monitors may have a relatively small processing power. The processes that demand the highest computational effort in this method are the calculation of the rms voltage profile and median filtering. As mentioned previously, PQ monitors are already able to compute the rms voltage profile in real-time, thus the only issue remaining to be analysed is their ability to perform fast median filtering. Even though a hardware implementation has not been done in this study, there are algorithms for recursive and fast median filtering computation [46, 47]. Therefore, this rms voltage step change detector is simple enough to be implemented in commercial PQ monitors.

5 Results of the Proposed Method

This section analyses the performance of the proposed filter in detecting rms voltage step changes in two datasets. In both cases, $p = 4$, $\delta_{step} = 0.0018$ pu, and $r = 3$ (see (16)). The parameter M is chosen such that the reference and observation windows cover the same amount of data samples as in the standard method discussed in Section 3.4, and therefore $M = 60$.

5.1 Dataset 1 - Field Data

The first dataset corresponds to voltage waveforms collected at the feeder head of a 25-kV, 60 Hz radial distribution system, immediately downstream the substation transformer. The power quality monitor collects 128 samples of voltage waveform data for each cycle. This dataset covers 28 minutes of continuous measurement and contains 8 rms voltage step changes caused by capacitor switching (4 energizing and 4 de-energizing operations).

The rms voltage profile for the entire monitoring interval, computed according to (1), is shown in Fig. 10a. This plot also shows the profile obtained through the filtering procedure proposed in this paper. Fig. 10b presents the respective rms voltage gradient, where one can observe that all rms voltage step changes have been successfully detected without any false-positives.

Figs. 11a and 11b represent the detailed view of the rms voltage profile around capacitor de-energizing and energizing operations, respectively. Note that the voltage fluctuations are not pr sent in the filtered profile and the abrupt step changes remain unaffected, as initially desired. As shown in Fig. 11b, in some instances, the unfiltered

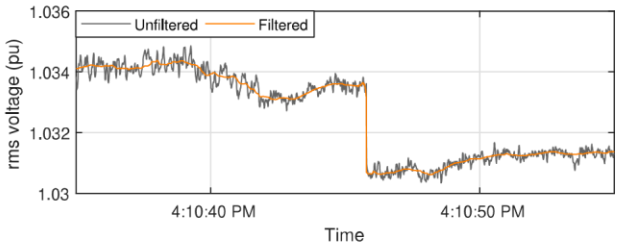

(a)

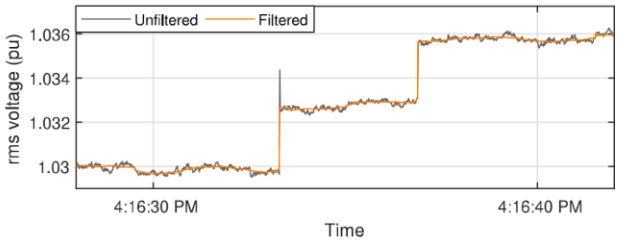

(b)

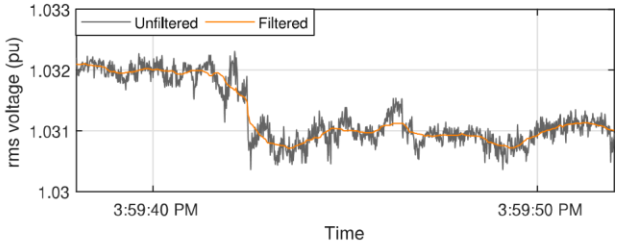

(c)

Fig. 11: Detailed view of the filtered rms voltage profile. (a) Capacitor de-energizing. (b) Capacitor energizing. (c) Load energizing.

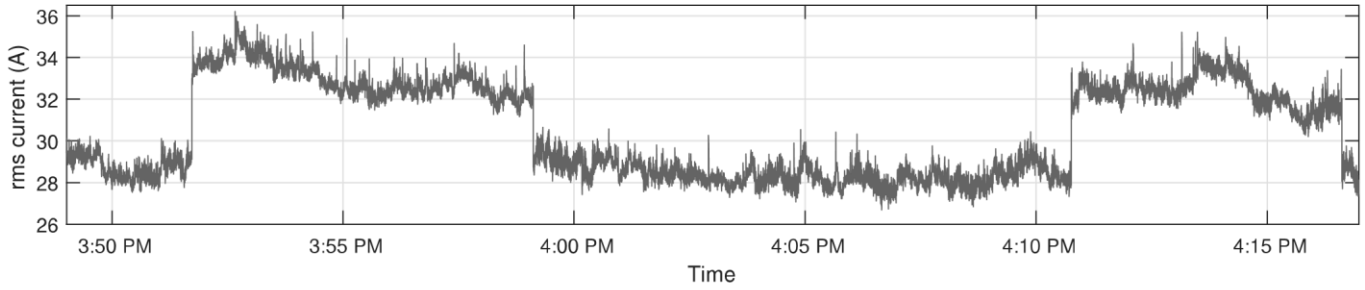

Fig. 12: Unfiltered rms current profile for the continuous field data measurement.

rms voltage profile contains spikes at the capacitor energizing instant due to the voltage waveform transients; these spikes are successfully removed by the proposed filter.

The rms voltage profile shows a small step change between 3:59 PM and 4:00 PM. Upon closer inspection, it was determined that the magnitude of this step change is about 0.001 pu only, as illustrated in Fig. 11c. This value does not exceed the threshold set by δ_{step}, and, therefore, this small step change is not detected. This relatively small rms voltage step change is caused by a load energizing operation; the power flow at the substation, computed through the voltage and current waveforms [48, 49], increases about 10 kVA at that instant.

The limitation on the use of current data is illustrated through this dataset, which contains data for the switching operations of both upstream and downstream capacitor banks. The relative capacitor location is defined as follows: a capacitor bank on the monitored feeder is downstream the power quality monitor, while a capacitor bank on any of the other parallel feeders or at the transmission network is upstream the monitor. The location of each capacitor bank relative to the monitoring point (i.e. the substation transformer) is determined by the measured reactive power flow, as this quantity is affected only if the capacitor bank is downstream the monitoring device [50]. Fig. 12 represents the unfiltered rms current profile, where 4 step changes are noticeable. The four additional steps changes observed in the rms voltage profile in Fig. 10a correspond to the switching of upstream capacitor banks, and therefore they cannot be observed in the rms current profile.

5.2 *Dataset 2 - Simulated Data*

The next analysis is performed on the rms voltage profile of the hypothetical scenario 2 presented in Section 3.4. In this case, the rms voltage linearly decreases from 1 pu to 0.996 pu over an interval of 1 second.

Fig. 13a shows the filtered rms voltage profile using either a three-stage median filter (adopting the same filter lengths suggested in Section 3.2) or the proposed filter. It is clear that only the proposed filter is able to successfully track the linearly varying rms voltage prior to the step change. Moreover, Fig. 13b illustrates that the step change is detected when the rms voltage gradient technique is applied to the rms voltage profile filtered by the proposed filter, but not with the three-stage median filter.

5.3 *Comparison with a Previous Approach*

A previous study employed the same unfiltered rms voltage profile depicted in Fig. 10a to detect subtle rms voltage step changes [33]. The method proposed in the previous study and the current approach have the same performance, i.e. all rms voltage step changes caused by capacitor switching operations are detected without any false-positive. The differences between the two methods are discussed below.

The previous study uses a combination of median and linear filters to obtain the filtered rms voltage profile. The filter choice at each time index is based on statistical tests (two-sample t-test and F-test for mean and variance equality, respectively), which assume that the rms voltage values converge to a normal distribution. The normality assumption has been verified to be true for multiple datas ts of field

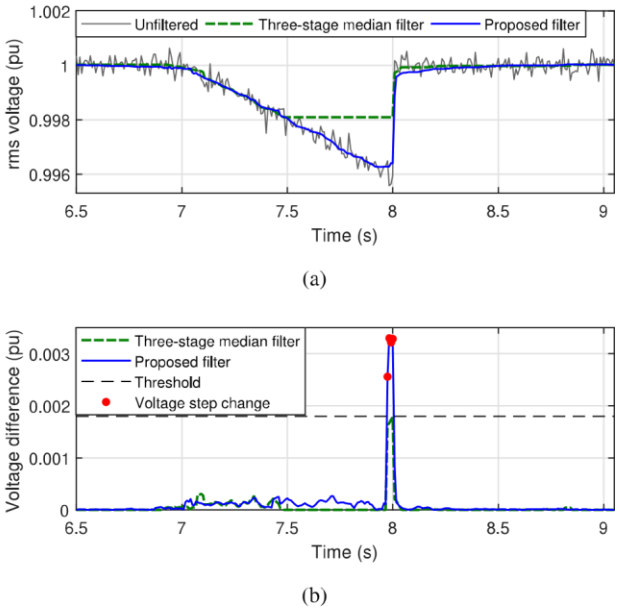

Fig. 13: RMS voltage step change detection using either a three-stage median filtering or the proposed technique. (a) RMS voltage profile. (b) RMS voltage gradient.

data through the Shapiro-Wilk test. However, there is no mathematical proof to assure that this strong assumption will always be true. On the other hand, the technique proposed in this paper does not depend on the underlying probability distribution of the rms voltage values.

Regarding the statistical tests described in the previous study, the user is required to set a significance level; a value of 5% was chosen in [33]. This value has no physical meaning, so that extensive prior analysis may be necessary for determining it. On the other hand, the threshold value used in this paper (δ_{step}) is obtained from the well-understood capacitor switching operations, as discussed in Section 3.3.1.

Finally, the previous study employs an adaptive technique for determining the threshold for rms voltage step change detection. This approach works without the need of setting a fixed threshold, which is an advantage. However, the algorithm requires a wait interval immediately after a step change detection to determine the new operating voltage level and the boundaries for normal operation; i.e., multiple successive step changes may not be detected if they occur within a short interval. The approach proposed in this paper does not have this limitation.

6 Conclusion

The novel filter proposed in this paper successfully attenuates the rapid voltage fluctuations in an rms voltage profile, without blurring out the abrupt step changes caused by switching events. It

IET Generation, Transmission & Distribution, pp. 1–10

was demonstrated that the shape of rms voltage profiles is useful for finding information about rms voltage step changes caused by either conspicuous (capacitor energizing) or inconspicuous (capacitor de-energizing) power quality disturbances. Therefore, these step changes in an rms voltage profile behave as an alternative triggering technique for continuously recorded PQ data. However, these triggering points are only an approximation and have a relatively low accuracy in relation to the true inception instant of the underlying event. This limitation is caused by the time resolution of the discrete rms voltage sequence, which is associated with the window size and refresh rate employed in the rms computation.

One application of the proposed rms voltage step change detector is as a power quality data mining and data reduction algorithm, where an abrupt variation in the rms voltage value represents a change in the steady-state conditions of the system. Once such variation has been detected, the instantaneous voltage and/or current waveforms are analysed in further detail (for example, through the computation of rms profiles with a 1-sample time resolution).

The method proposed in this paper was able to detect all rms voltage step changes caused by capacitor switching operations without any false-positive detection for a dataset including voltage waveforms recorded continuously for 28 minutes. Moreover, it was shown that the proposed technique correctly detects rms voltage step changes even if the system is not in quasi-steady-state before their occurrence, as illustrated through field and simulated data. Even though this paper focused on capacitor switching events, the proposed detector is applicable to any PQ disturbance accompanied by rms voltage step changes.

7 References

1 Silva, L., Kapisch, E., Martins, C., Filho, L., Cerqueira, A., Duque, C., et al.: 'Gapless power-quality disturbance recorder', *IEEE Transactions on Power Delivery*, 2017, **32**, (2), pp. 862–871

2 Li, B., Jing, Y., Xu, W.: 'A generic waveform abnormality detection method for utility equipment condition monitoring', *IEEE Transactions on Power Delivery*, 2017, **32**, (1), pp. 162–171

3 Lieberman, D.G., Troncoso, R.J.R., Rios, R.A.O., Perez, A.G., Yepez, E.C.: 'Techniques and methodologies for power quality analysis and disturbances classification in power systems: a review', *IET Generation, Transmission and Distribution*, 2011, **5**, (4), pp. 519–529

4 Demirci, T., Kalaycioglu, A., Kucuk, D., Salor, O., Guderl, M., Pakhuylu, S., et al.: 'Nationwide real-time monitoring system for electrical quantities and power quality of the electricity transmission system', *IET Generation, Transmission and Distribution*, 2011, **5**, (5), pp. 540–550

5 Broshi, A. 'Monitoring power quality beyond EN 50160 and IEC 61000-4-30'. In: Proc. IEEE Power Engineering Society Conference and Exposition in Africa - PowerAfrica, 2007, pp. 1–7

6 De, S., Debnath, S.: 'Real-time cross-correlation-based technique for detection and classification of power quality disturbances', *IET Generation, Transmission and Distribution*, 2018, **12**, (3), pp. 688–695

7 Bastos, A.F., Santoso, S. 'Identifying switched capacitor relative locations and energizing operations'. In: Proc. IEEE Power and Energy Society General Meeting, 2016, pp. 1–5

8 Bollen, M., Gu, I.: 'Signal Processing of Power Quality Disturbances'. (Hoboken, NJ: Wiley, 2006)

9 Lima, E.M., Junqueira, C.M.S., Brito, N.S.D., Souza, B.A., Coelho, R.A., Medeiros, H.G.M.S.: 'High impedance fault detection method based on the short-time Fourier transform', *IET Generation, Transmission and Distribution*, 2018, **12**, (11), pp. 2577–2584

10 Eristi, H., Demir, Y.: 'Automatic classification of power quality events and disturbances using wavelet transform and support vector machines', *IET Generation, Transmission and Distribution*, 2012, **6**, (10), pp. 968–976

11 Santoso, S., Powers, E.J., Grady, W.M., Parsons, A.C.: 'Power quality disturbance waveform recognition using wavelet-based neural classifier - part 1: Theoretical foundation', *IEEE Transactions on Power Delivery*, 2000, **15**, (1), pp. 222–228

12 Tripathy, L., Samantaray, S.R., Dash, P.K.: 'Sparse S-transform for location of faults on transmission lines operating with unified power flow controller', *IET Generation, Transmission and Distribution*, 2014, **9**, (15), pp. 2108–2116

13 Ashrafian, A., Rostami, M., Gharehpetian, G.B.: 'Hyperbolic S-transform-based method for classification of external faults, incipient faults, inrush currents and internal faults in power transformers', *IET Generation, Transmission and Distribution*, 2012, **6**, (10), pp. 940–650

14 Gil, M., Abdoos, A.A.: 'Intelligent busbar protection scheme based on combination of support vector machine and S-transform', *IET Generation, Transmission and Distribution*, 2017, **11**, (8), pp. 2056–2064

15 Duque, C.A., Ribeiro, M.V., Ramos, F.R., Szczupak, J.: 'Power quality event detection based on the divide and conquer principle and innovation concept', *IEEE Transactions on Power Delivery*, 2005, **20**, (4), pp. 2361–2369

16 Kose, N., Salor, O., Leblebicioglu, K.: 'Kalman filtering based approach for light flicker evaluation of power systems', *IET Generation, Transmission and Distribution*, 2010, **5**, (1), pp. 57–69

17 Xi, Y., Li, Z., Zeng, X., Tang, X., Zhang, X., Xiao, H.: 'Fault location based on travelling wave identification using an adaptive extended Kalman filter', *IET Generation, Transmission and Distribution*, 2018, **12**, (6), pp. 1314–1322

18 Ghanbari, T.: 'Kalman filter based incipient fault detection method for underground cables', *IET Generation, Transmission and Distribution*, 2015, **9**, (14), pp. 1988–1997

19 Jin, T., Liu, S., Flesch, R.C.C.: 'Mode identification of low-frequency oscillations in power systems based on fourth-order mixed mean cumulant and improved TLS-ESPRIT algorithm', *IET Generation, Transmission and Distribution*, 2017, **11**, (15), pp. 3739–3748

20 Dafis, C.J., Nwankpa, C.O., Petropulu, A. 'Analysis of power system transient disturbances using an ESPRIT-based method'. In: Proc. Power Engineering Society Summer Meeting, 2000, pp. 437–442

21 Gu, I.Y.H., Styvaktakis, E., Bollen, M.H.J.: 'Analyzing power disturbances using the residuals of AR models', *IEEE Power Engineering Review*, 2000, **20**, (4), pp. 60–62

22 Gu, I.Y.H., Styvaktakis, E.: 'Bridge the gap: signal processing for power quality applications', *Electric Power Systems Research*, 2003, **66**, (1), pp. 83–96

23 Carpinelli, G., Chiodo, E., Lauria, D.: 'Indices for the characterisation of bursts of short-duration waveform distortion', *IET Generation, Transmission and Distribution*, 2007, **1**, (1), pp. 170–175

24 Bastos, A.F., Lao, K.W., Todeschini, G., Santoso, S.: 'Accurate identification of point-on-wave inception and recovery instants of voltage sags and swells', *IEEE Transactions on Power Delivery*, 2018 (Early Access), **-**, (-), pp. –

25 Radil, T., Ramos, P.M., Janeiro, F.M., Serra, A.C.: 'PQ monitoring system for real-time detection and classification of disturbances in a single-phase power system', *IEEE Transactions on Instrumentation and Measurement*, 2008, **57**, (8), pp. 1725–1733

26 IEC 61000-4-30. 'IEC Electromagnetic Compatibility: Testing and measurements techniques - Power quality measurement methods', 2015.

27 IEEE Std. 1564. 'IEEE Guide for Voltage Sag Indices', 2014.

28 Balouji, E., Salor, O.: 'Digital realisation of the IEC flickermeter using root mean square of the voltage waveform', *IET Generation, Transmission and Distribution*, 2016, **10**, (7), pp. 1663–1670

29 Bastos, A.F., Santoso, S., Todeschini, G. 'Comparison of methods for determining inception and recovery points of voltage variation events'. In: Proc. IEEE Power and Energy Society General Meeting, 2018, pp. 1–5

30 Gustafsson, F.: 'Adaptive Filtering and Change Detection'. (John Wiley & Sons, 2000)

31 Smith, S.: 'The Scientist and Engineer Guide to Digital Signal Processing'. (San Diego: California Tech. Pub., 1997)

32 Castro, E.A., Donoho, D.L.: 'Does median filtering truly preserve edges better than linear filtering?', *The Annals of Statistics*, 2009, **37**, (3), pp. 1172–1206

33 Bastos, A.F., Lao, K.W., Todeschini, G., Santoso, S.: 'Novel moving average filter for detecting rms voltage step changes in triggerless PQ data', *IEEE Transactions on Power Delivery*, 2018, **33**, (6), pp. 2920–2929

34 Nguyen, T.T., Li, X.J.: 'Application of a z-transform signal model and median filtering for power system frequency and phasor measurements', *IET Generation, Transmission and Distribution*, 2007, **1**, (1), pp. 72–79

35 Huber, P.J.: 'Robust estimation of a location parameter', *The Annals of Mathematical Statistics*, 1964, **35**, (1), pp. 73–101

36 Abarghouei, H.F., Nayeripour, M., Hasanvand, S., Waffenschmidt, E.: 'Online hierarchical and distributed method for voltage control in distribution smart grids', *IET Generation, Transmission and Distribution*, 2017, **11**, (5), pp. 1223–1232

37 Short, T.A.: 'Electric Power Distribution Handbook'. (CRC Press, FL: Boca Raton, 2003)

38 IEEE Std. 1036. 'IEEE Guide for Application of Shunt Power Capacitors', 2010.

39 Bassseville, M., Nikiforov, I.V.: 'Detection of Abrupt Changes: Theory and Application'. (Englewood Cliffs, NJ: Prentice Hall, 1993)

40 Davies, P.L., Gather, U.: 'The breakdown point - examples and counterexamples', *Statistical Journal*, 2007, **5**, (1), pp. 1–17

41 Maronna, R.A., Martins, R.D., Yohai, V.J.: 'Robust Statistics: Theory and Methods'. (John Wiley & Sons, 2006)

42 Rousseeuw, P.J., Croux, C.: 'Alternatives to the median absolute deviation', *Journal of the American Statistical Association*, 1993, **88**, (424), pp. 1273–1283

43 Pearson, R.: 'Outliers in process modeling and identification', *IEEE Transactions on Control Systems Technology*, 2002, **10**, (1), pp. 55–63

44 Leys, C., Klein, O., Bernard, P., Licata, L.: 'Detecting outliers: Do not use standard deviation around the mean, use absolute deviation around the median', *Journal of Experimental Social Psychology*, 2013, **49**, (4), pp. 746–766

45 Carnovale, D., Ellis, D.: 'Mind your P's and Q's', *IEEE Industry Applications Magazine*, 2003, **9**, (2), pp. 55–63

46 Zhang, Q., Xu, L., Jia, J. '100+ times faster weighted median filter (WMF)'. In: IEEE Conference on Computer Vision and Pattern Recognition, 2014, pp. 2830–2837

47 Perreault, S., Hebert, P.: 'Median filtering in constant time', *IEEE Transactions on Image Processing*, 2007, **16**, (9), pp. 2389–2394

48 Bastos, A.F., Biyikli, L., Santoso, S. 'Analysis of power factor over correction in a distribution feeder'. In: Proc. IEEE/PES Transmission and Distribution Conference and Exposition, 2016, pp. 1–5

49 Rodriguez, M.V., Troncoso, R.J.R., Perez, A.G., Lieberman, D.G., Rios, R.A.O.: 'Reconfigurable instrument for neural-network based power-quality monitoring in 3-phase power systems', *IET Generation, Transmission and Distribution*, 2013, **7**, (12), pp. 1498–1507

50 Hur, K., Santoso, S.: 'On two fundamental signatures for determining the relative location of switched capacitor banks', *IEEE Transactions on Power Delivery*, 2008, **23**, (2), pp. 1105–1112